21st Australasian Fluid Mechanics Conference
Adelaide, Australia
10-13 December 2018

Pressure Boundary Condition Investigation for Side Branch in Coronary Bifurcation Simulations

B. Jiang[1], E.K.W. Poon[1], S.J. Illingworth[1], P. Barlis[1,2] and A.S.H. Ooi[1]

[1]Department of Mechanical Engineering, Melbourne School of Engineering
The University of Melbourne, Victoria 3010, Australia

[2]Melbourne Medical School, Faculty of Medicine, Dentistry & Health
The University of Melbourne, Victoria 3010, Australia

Abstract

Computational fluid dynamics (CFD) research tools have been widely used to investigate the complex hemodynamic behaviour at coronary bifurcations. To quantify the coronary flow distribution at the bifurcation, a scaling law is used to calculate flow rate distribution based on diameter ratio of the side branch (SB) and the distal main vessel. In this case, velocity is often used as the boundary condition at the outlets. However, velocity boundary condition often requires careful treatments of the arterial geometries at the outlets (e.g., extend the outlet, regulate imperfect cross-sectional shapes), which may increase computational demand significantly. Comparing to velocity, pressure is nearly constant across the cross section and does not depend on the shape of the cross section (assuming the boundary is at a certain distance away from the bifurcation). In this study, we investigate the implications of employing pressure boundary conditions at the outlets that would achieve identical flow rate distribution as depicted by the scaling law. Idealized bifurcation geometries with different bifurcation angles (BA) and SB diameters were created. The vessel diameters are chosen based on population mean values. In all cases, the cross-sectional pressure contour becomes uniform in the SB within 15 mm from the ostium, while velocity profile is not fully developed until approximately 40 mm from the ostium. This study aims to provide the essential pressure boundary conditions that mimic the physiological flow distributions for different coronary bifurcation configurations. Ultimately, these pressure boundary conditions would improve the accuracy of future patient-specific CFD studies.

Introduction

Coronary arterial bifurcations are prone to atherosclerosis development due to their relatively complicated geometry and haemodynamic environment. Percutaneous coronary interventions performed at bifurcation regions consist 15% - 20% of the total number [1]. Computational fluid dynamics (CFD) research tools have been widely used to investigate the complex flow behaviour at the bifurcation. Coronary flow distributions into the main vessel and side branch(es) (SB) often depends on the myocardial demands downstream. A scaling law can be applied to determine the flow distribution to the SB and distal main vessel. Murray was the first to derive the theoretical scaling law between the flow rate and the diameter with the power of three ($Q_2/Q_1 = (D_2/D_1)^3$, where the subscripts 2 and 1 refers to the SB and the distal main vessel respectively), based on minimal energy consumption [2]. However, clinical research have shown that Murray's law underestimates flow into SB [3]. van der Giessen et al. obtained the power number of 2.27, $(Q_2/Q_1 = (D_2/D_1)^{2.27}$, by fitting clinical measurement of 21 patients under various coronary diseases [3,4]. This scaling law is used by many current studies [4–7]. These studies applied velocity boundary condition to achieve the exact flow rate as depicted by the scaling law.

Velocity boundary condition often requires careful treatments at the outlets such as using a parabolic velocity profile, merging the patient SB with circular cross-section, and extending the outlet to achieve fully developed flow. In patient specific coronary bifurcation reconstruction, cross section of the coronary artery is unlikely to be a perfect circle, and thus it becomes difficult to specify the exact velocity profile at the correspondent location. In other words, defining a velocity distribution as an outlet boundary condition may result unrealistic flow. This may be offset by extending the length of the coronary artery SB. However, such a methodology will significantly increase computational demand, as the length required for a fully developed laminar pipe flow is approximately $0.05Re{\cdot}D$, where Re is the Reynold's number based on diameter D.

Pressure boundary condition has several advantages over velocity boundary condition. Pressure is nearly constant across the cross section and it does not depend on the shape of the cross section, and thus it reduces the efforts to modify the imperfect outlet. Pressure usually reaches homogeneous condition at a much closer axial location than velocity, which means, potentially, pressure boundary can be applied in cases with much shorter vessel length distal to bifurcation. Therefore, by applying pressure boundary condition, computational demand could be decreased significantly, and cases with irregular vessel cross-sections is suitable for pressure boundary condition. In this study, pressure distribution is systematically investigated by varying the bifurcation angle (BA) and the SB diameter. The results obtained could be used as pressure boundary condition in studies of bifurcation simulations with similar geometry.

Method

In this study, the effects of various BAs and diameters of SB are investigated. As shown in Figure 1, the main vessel inlet diameter and the diameter of the distal main vessel are kept constant as 4.5 and 3.5 mm respectively. The diameter of the bifurcation has three settings: 3.5, 2.8 and 2.1 mm, and the BA values are 40°, 60°, 80° and 100°. Therefore, by parametric studying the three diameters and four degrees, a total of twelve cases are simulated. The vessel lengths of the distal main vessel and the SB are both 60 mm measured from the bifurcation centre to the distal ends.

Blood flow is assumed to be steady, and the inlet boundary condition is fixed flow rate of (2.8 ml/s) for all cases [8], and the flow rate through the SB is calculated based on the scaling law, $Q_1/Q_2 = (R_1/R_2)^{2.27}$ [4]. The outlet of the distal main vessel has a zero-pressure boundary condition. Blood is assumed to be Newtonian with dynamic viscosity $\mu = 3.3\times10^{-3}$ Pa·s, and density $\rho = 1060$ kg/m^3. The mesh is generated in Pointwise (v. 18.0, Pointwise, Inc., Fort Worth, TX) using tetrahedral elements, and prism layers are generated at the near wall region to capture the high velocity gradient. The total number of cells

in each case is approximately 2 million, a grid independence test is performed by quadrupling the cell number and the difference in velocity at the vessel centreline is less than 1%. CFD simulations are carried out by directly solving the incompressible Navier–Stokes equations using an open source CFD software OpenFOAM-2.1.1 (OpenCFD Ltd., ESI group, Bracknell, UK).

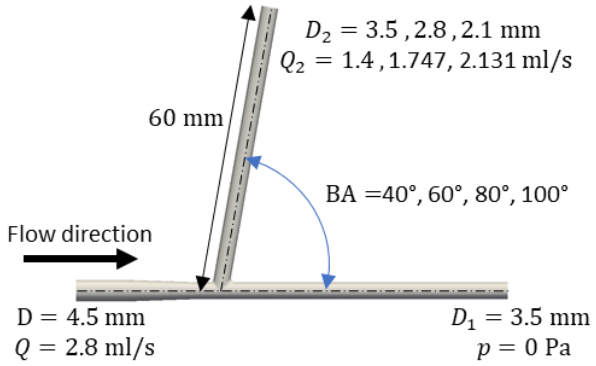

Figure 1 Model geometry and boundary conditions

Results and discussion

The case of BA = 80° and D_2 = 3.5 mm is used as a demonstration as this BA and diameter are population average values of the left main bifurcation [9,10]. Figure 2 shows the velocity and pressure profile changes distal to the bifurcation. Velocity and pressure are extracted at 5 mm intervals along the distal main vessel and the SB. From the inset in Figure 2, both velocity and pressure profile are skewed at 5 mm axial location distal to the bifurcation. However, the velocity distribution has not reached a fully developed condition until 35 mm to 40 mm, while the pressure is uniform at about 10 mm distal to bifurcation.

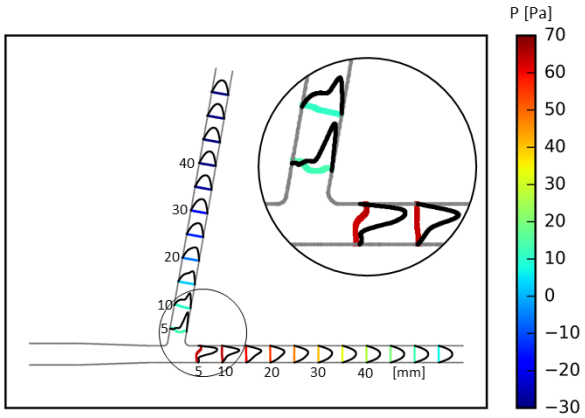

Figure 2 Velocity and pressure profile plotted at different axial location. A zoom-in of the bifurcation region is shown in the inset.

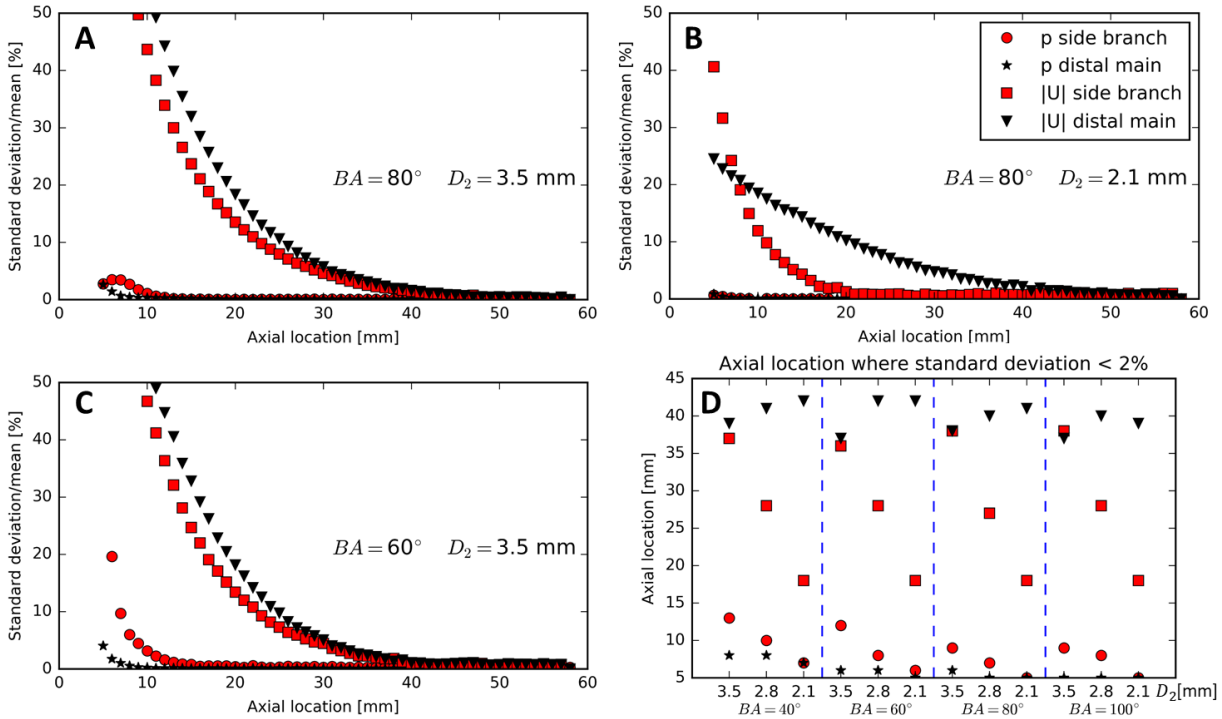

Figure 3 (A, B, C) Standard deviation/mean of velocity and pressure cross-sectional profile along the axial direction of the distal main and the SB. (D) The axial locations of velocity and pressure where standard deviation drops below 2%.

Figure 3 shows standard deviation/mean of velocity and pressure cross-sectional profile along the axial direction of the distal main and the SB. The percentage is calculated by $\mathrm{std}(U')/U_{\mathrm{mean}} \times 100$, where std() is standard deviation, and U' is local velocity profile offset from the developed profile. Pressure standard deviation in percentage is calculated in the same method $\mathrm{std}(P')/P_{\mathrm{mean}} \times 100$. It shows the severity of fluctuation of the local profile compared to the developed profile, which indicates how fast the velocity and pressure develop. To clearly demonstrate the trend, only the cases of BA=80° and 100° are used. The other cases follow the same

trend. For Figure 3A and Figure 3C, the diameters are kept constant while the BA decreases. The pressure standard deviation is relatively high at the near bifurcation region (5 to 10 mm), especially in the SB (20%). As the BA decreases from 80° to 60°, the pressure profile becomes more skewed at the 5 mm location. On the contrary, the velocity is less sensitive to BA changes. As shown in Figure 3A to 3B, the pressure deviation further decreases as the SB diameter decreases while the BA decreases. The distance to acquire a fully developed velocity profile is significantly affected by the change of diameter in the SB. In the distal main vessel of Figure 3A and Figure 3B, at ~5 mm distal to the bifurcation, the velocity deviation drops from over 50% to 22%, but the distance to reach developed state is around 37 to 39 mm. While the velocity in the SB converges much faster as the diameter decreases. Figure 3D summarises all the distances required in each case to achieve uniform pressure distribution and fully develop velocity profile (< 2% standard deviation/mean). Uniform pressure distribution is achieved within 15 mm length from the coronary bifurcation in all the cases. Therefore, to use the pressure boundary condition, a safe vessel length after bifurcation is longer than 15 mm.

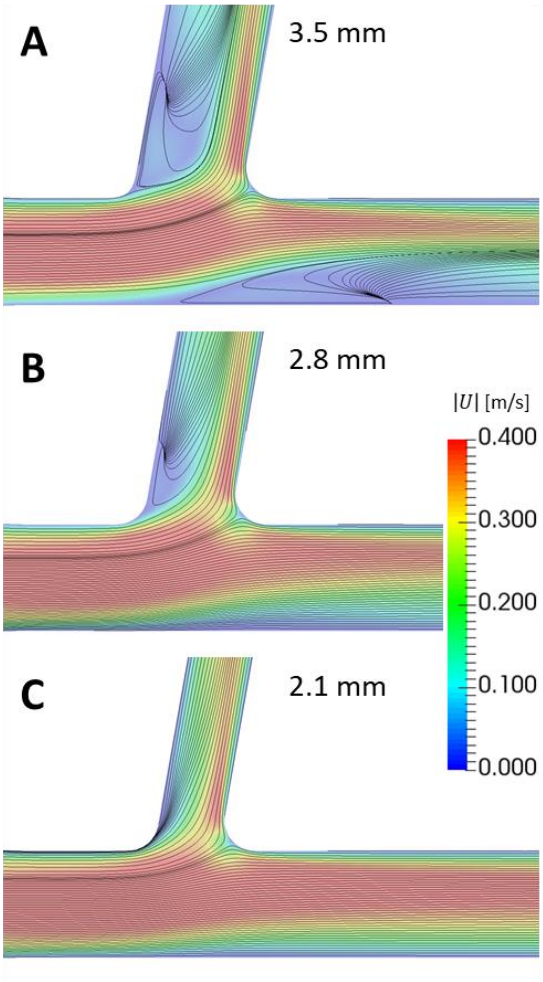

Figure 4 2D projected streamlines and velocity contours at coronary artery bifurcation for various SB diameters: (A) SB diameter = 3.5 mm; (B) 2.8 mm and (C) 2.1 mm.

Figure 4 shows the streamlines at the bifurcation region of the cases BA=80° with different SB diameters. In Figure 4A, where the SB diameter is 3.5 mm which is equal to the distal main diameter. Recirculation bubbles are observed in both SB and the distal main vessel near the bifurcation. On the other hand, as the diameter of the SB decreases, the recirculation bubble firstly disappears in the distal main vessel. And with a further reduction in the SB diameter, the recirculation bubble also disappears in the SB. The cases with other BAs follow the same trend, with slight changes in the recirculation bubble size.

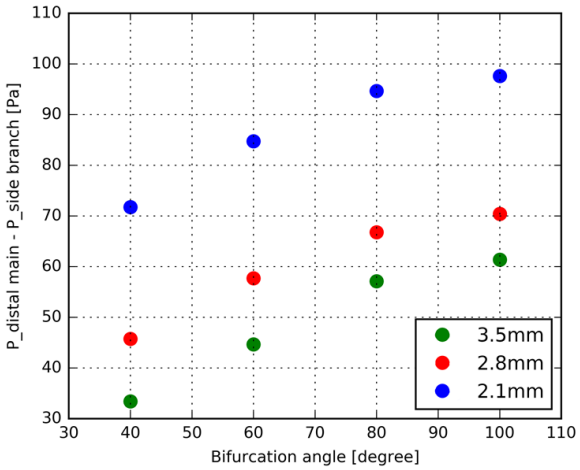

Figure 5 The pressure difference between the distal main vessel and the SB at location of 15 mm distal to bifurcation centre.

Figure 5 shows the pressure difference between the distal main vessel and the SB. To ensure the pressure has reached a uniform profile, the pressure values are taken at a safe distance of 15 mm from the bifurcation centre. This information can be used to apply pressure boundary conditions for the outlets in similar geometries. The trend is clear in the figure that the pressure difference increases as the BA increases and it also increases as the SB diameter decreases (from 3.5 to 2.1 mm). The trend of every data set (same diameter, various BA) are similar to each other, but with a shift up in pressure difference. This implies that the diameter change causes the pressure difference shifting. Therefore, BA and SB diameter are independent variables of the pressure difference between the distal main vessel and the SB.

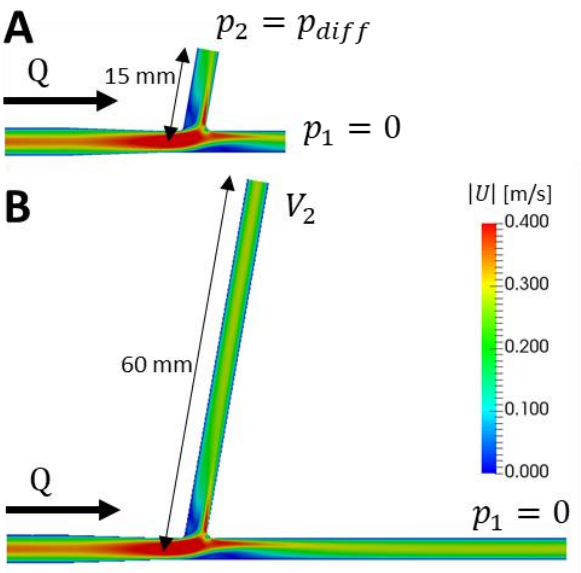

Figure 6 Velocity distribution comparison of the cases with pressure boundary conditions and velocity boundary conditions. (A) Shortened vessels (15 mm) with a pressure boundary condition, the pressure at the SB outlet is set to be the pressure difference between the distal main

vessel and the SB at 15 mm location distal to the bifurcation. (B) Original simulation with velocity boundary condition at the SB outlet.

As shown in Figure 6, the pressure difference of the case BA=80°, D_2=3.5 mm is used to set the boundary condition of the same geometry at the bifurcation but with a shorter vessel length (15 mm) to study the accuracy of the pressure boundary condition. The velocity distribution is shown in Figure 6A to compare to the original result in Figure 6B with a velocity boundary condition at the SB outlet. The velocity flow through the SB is 3.4% more in the pressure boundary condition case than the velocity condition case. Furthermore, based on the same mesh quality and computing resource, the computational time consumption in the pressure boundary case is only one fifth of the original velocity boundary condition case.

Conclusions

In this study, pressure is found to be more homogeneous than velocity, which requires shorter distance to develop. Larger BAs and thinner vessels decrease the distance needed for the pressure to become uniform. The pressure difference between the distal main vessel and the SB increases with thinner SBs and also with increasing BAs. In steady blood flow simulations with bifurcations, a proper pressure boundary condition with 15 to 20mm of vessel length is sufficient to achieve accurate velocity distributions and to study the hemodynamic behaviour at the bifurcation region. In this setup, the cases with pressure boundary conditions can potentially save significant computational resources.

References

[1] Lassen, J. F., Holm, N. R., Banning, A., Burzotta, F., Lefèvre, T., Chieffo, A., Hildick-Smith, D., Louvard, Y., and Stankovic, G., 2016, "Percutaneous Coronary Intervention for Coronary Bifurcation Disease: 11th Consensus Document from the European Bifurcation Club," EuroIntervention, **12**(1), pp. 38–46.

[2] Murray, C. D., 1926, "The Physiological Principle of Minimum Work: I. The Vascular System and the Cost of Blood Volume," Proc. Natl. Acad. Sci., **12**(3), pp. 207–214.

[3] Doriot, P., Dorsaz, P., Dorsaz, L., De Benedetti, E., Chatelain, P., and Delafontaine, P., 2000, "In-Vivo Measurements of Wall Shear Stress in Human Coronary Arteries.," Coron. Artery Dis., **11**(6), pp. 495–502.

[4] van der Giessen, A. G., Groen, H. C., Doriot, P. A., de Feyter, P. J., van der Steen, A. F. W., van de Vosse, F. N., Wentzel, J. J., and Gijsen, F. J. H., 2011, "The Influence of Boundary Conditions on Wall Shear Stress Distribution in Patients Specific Coronary Trees," J. Biomech., **44**(6), pp. 1089–1095.

[5] Chiastra, C., Gallo, D., Tasso, P., Iannaccone, F., Migliavacca, F., Wentzel, J. J., and Morbiducci, U., 2017, "Healthy and Diseased Coronary Bifurcation Geometries Influence Near-Wall and Intravascular Flow: A Computational Exploration of the Hemodynamic Risk," J. Biomech., **58**(2017), pp. 79–88.

[6] Gijsen, F. J. H., Schuurbiers, J. C. H., van de Giessen, A. G., Schaap, M., van der Steen, A. F. W., and Wentzel, J. J., 2014, "3D Reconstruction Techniques of Human Coronary Bifurcations for Shear Stress Computations," J. Biomech., **47**(1), pp. 39–43.

[7] Chiastra, C., Morlacchi, S., Gallo, D., Morbiducci, U., Cárdenes, R., Larrabide, I., and Migliavacca, F., 2013, "Computational Fluid Dynamic Simulations of Image-Based Stented Coronary Bifurcation Models.," J. R. Soc. Interface, **10**(84), p. 20130193.

[8] Kim, H. J., Vignon-Clementel, I. E., Coogan, J. S., Figueroa, C. A., Jansen, K. E., and Taylor, C. A., 2010, "Patient-Specific Modeling of Blood Flow and Pressure in Human Coronary Arteries," Ann. Biomed. Eng., **38**(10), pp. 3195–3209.

[9] Pflederer, T., Ludwig, J., Ropers, D., Daniel, W. G., and Achenbach, S., 2006, "Measurement of Coronary Artery Bifurcation Angles by Multidetector Computed Tomography.," Invest. Radiol., **41**(11), pp. 793–8.

[10] Dodge, J. T., Brown, B. G., Bolson, E. L., and Dodge, H. T., 1992, "Lumen Diameter of Normal Human Coronary Arteries. Influence of Age, Sex, Anatomic Variation, and Left Ventricular Hypertrophy or Dilation.," Circulation, **86**(1), pp. 232–246.

.